Int. J. Electron. Commun. (AEÜ) 67 (2013) 926–936

Contents lists available at SciVerse ScienceDirect

International Journal of Electronics and Communications (AEÜ)

journal homepage: www.elsevier.com/locate/aeue

Detection of interdependent primary systems using wideband cognitive radios

Burak Yılmaz, Serhat Erküçük*

Department of Electrical and Electronics Engineering, Kadir Has University, Fatih, 34083 İstanbul, Turkey

ARTICLE INFO

Article history:
Received 14 November 2012
Accepted 8 May 2013

Keywords:
Cognitive radios
Ultra wideband (UWB) systems
Detect-and-avoid (DAA)
Wideband spectrum sensing
Energy detection

ABSTRACT

Cognitive radios (CRs) may be sharing multiple frequency bands with primary systems if the CR is a wideband or an ultra wideband (UWB) system. In that case, the CR should ensure all the coexisting primary systems in these bands are detected before it can start data transmission. In this work, we study the primary system detection performance of a wideband CR assuming that there are multiple coexisting primary systems and that these primary systems may be *jointly active*. Accordingly, we consider the implementation of energy detection scheme in multiple bands followed by two detection methods: (i) a maximum-a-posteriori (MAP) based detection (i.e., joint detection) that takes into account the statistics of simultaneously operating systems in independent bands and (ii) a Neyman–Pearson (NP) test based detection that optimizes the threshold values independently in each band (i.e., independent detection). For a simpler implementation of the independent detection, we show that the threshold values obtained from joint detection can be used in order to achieve the optimum NP test based independent detection results. In addition to quantifying the gain of joint detection over independent detection in terms of probabilities of false alarm and detection for practical scenarios, we also present the operation capability of CRs in terms of the fractions of time the CR can access the channel without interfering with the primary systems. The results are important for the practical implementation of multiband detection when the primary systems are known to be interdependent.

1. Introduction

As a result of increased demand for new wireless communication technologies, there have been numerous licensed systems assigned to different frequency bands in recent years. This has caused the spectrum become very crowded, and yet not well utilized. In the last decade cognitive radios (CRs) [1] and ultra wideband (UWB) systems [2] have been proposed and investigated as unlicensed systems, where they have been widely accepted as alternative technologies for better utilization of the spectrum. From the perspective of a licensed primary system, the major concern for the implementation of either CRs or UWB systems is the possible interference they may cause to primary systems. Hence, many regulatory agencies worldwide have mandated detect-and-avoid (DAA) techniques in various bands [3]. Accordingly, CRs and UWB systems have to perform spectrum sensing in these bands before they can communicate.

Spectrum sensing has been widely explored in the context of cognitive radios. Surveys of existing spectrum sensing techniques can be found in [4] and [5]. While some techniques are based on matched filtering or feature detection of primary users' signals, energy detection [6] is the most common technique because of its low computational and implementation complexity in addition to not requiring any knowledge of the primary users' signals, despite the challenges in signal detection reliability for a low signal-to-noise ratio (SNR) [4]. There is a comprehensive literature on energy detection in a single frequency band with further improvements using collaboration among secondary users [7–9], diversity schemes [10], multiple antennas [11] and a model considering the primary user appearance probability [12].

On the other hand, the literature on energy detection in multiple frequency bands is rather new. This concept is indeed quite important as it is more desired to assess the availability of a wider spectrum for better utilization. Moreover, the CRs may be wideband or UWB systems, and therefore, they should ensure all the coexisting primary systems in common bands are detected before they can start data transmission. In [13], the effect of number of primary users in different bands on the detection performance was investigated. In [14], the aggregate opportunistic throughput was maximized over multiple bands subject to some constraints on the amount of interference to primary users. In [15], soft and hard fusion techniques were considered to improve the detection performance in the presence of multiple secondary users. In [16], periodic sensing was added to the system model of [14] in order to improve the detection performance. The common assumption in

* Corresponding author. Tel.: +90 212 5336532.
E-mail addresses: burak.yilmaz@khas.edu.tr (B. Yılmaz), serkucuk@khas.edu.tr (S. Erküçük).

1434-8411/$ – see front matter © 2013 Elsevier GmbH. All rights reserved.
http://dx.doi.org/10.1016/j.aeue.2013.05.003

these studies was that the primary systems in different bands were independent. However, if the licensed systems in different bands are dependent, the detection performance can be further improved. In [17], the primary system detection performance was assessed for $M=2$ interdependent bands using a maximum-a-posteriori (MAP) based detection method and the detection gain over independent detection was quantified. However, this work was limited to $M=2$ bands.

In this paper, motivated by quantifying the detection performance gain when there are $M>2$ interdependent systems, we generalize the work in [17] to multiple bands. Here, $M>2$ could be an example of M systems in independent frequency bands with known activity statistics. For example, the statistics might indicate that two of the three systems are jointly active 40% of the time, while all three systems are jointly active 50% of the time and passive 10% of the time. For that we consider the implementation of energy detection scheme in multiple bands followed by either a MAP based detection (i.e., joint detection) or a Neyman–Pearson (NP) test based detection that optimizes the threshold values independently in each band (i.e., independent detection). Different from [17], the contribution of the current study is fourfold. Accordingly, we

1 generalize the probability of false alarm and detection expressions for $M>2$ for both joint and independent detection,
2 use the threshold values obtained from joint detection so as to achieve the optimum NP test based independent detection results with a simpler implementation,
3 provide practical examples to quantify the performance gain of joint detection over independent detection for various scenarios, and
4 present the operation capability of CRs as an additional performance measure in terms of the fractions of time the CR can access the channel without interfering with the primary systems.

In this work, in addition to generalizing the probability of false alarm and detection expressions [18], the accurate modeling of the decision variable with χ^2 distribution is discussed. This is important as most studies consider the approximate Gaussian distribution in their models. Using the χ^2 distribution in MAP based detection, joint detection analytical expressions and the associated threshold values are derived and presented in detail. While the commonly used performance measures are probabilities of false alarm and detection in the literature, the operation capability of CRs is introduced as an additional performance measure in this study. This is an important performance measure as CRs with similar detection performances may indeed utilize the common band quite differently depending on system activity values. Accordingly, the models and the results presented in this study are important for the practical implementation of multiband detection when there are multiple primary systems that are known to be interdependent.

The rest of the paper is organized as follows. In Section 2, the receiver model of the CR is presented. In Section 3, implementations of joint detection and independent detection are presented. In Section 4, numerical and simulation results are provided for the comparison of the considered detection methods under different scenarios. Concluding remarks are given in Section 5.

2. Receiver model

We assume that there are M primary systems operating in orthogonal frequency bands and coexisting with a wideband CR. Each primary system is assumed to communicate by transmitting a primary signal, $s_m(t)$, where each system has a bandwidth of W_m, $m=\{1,2,\ldots,M\}$. These systems may be active or passive depending on the time of the day. The received signals are filtered using ideal zonal bandpass filters with bandwidths W_m at each orthogonal frequency band to eliminate the out-of-band noise [6,10]. Accordingly, the two hypotheses corresponding to the absence and presence of the filtered signal received from the mth system, respectively, are

$$H_{0,m}: \quad r_m(t) = n_m(t) \tag{1}$$

$$H_{1,m}: \quad r_m(t) = A_m\, e^{j\theta_m}\, s_m(t-\tau_m) + n_m(t), \tag{2}$$

where each primary signal $s_m(t)$ passes through a channel with amplitude A_m and phase θ_m uniformly distributed over $[0, 2\pi)$, τ_m is the timing offset between the two systems, $n_m(t)$ is band-limited additive white Gaussian noise (AWGN) with variance $\sigma^2_{n_m} = N_0 W_m$ and $N_0/2$ is the two-sided noise power spectral density. Note that the channels are assumed to be frequency nonselective for the mth system, however, each system may have different attenuation values in each frequency band, which is the main critical assumption in our system model (i.e., different SNR levels in different bands).

In practice, timing offset is an important degradation factor on the detection performance. There are two major causes for timing offset: (i) asynchronism between users and (ii) asynchronism with the received signal. The first one occurs when there are multiple primary users in the same frequency band. If the primary signals communicate with timing misalignment, this may cause decreased spectrum opportunities [19]. The second one occurs when the receiver is not synchronized with the received signal, where the signal of interest may arrive at the CR receiver while the CR is already sensing the spectrum [20]. In that case, the observed signal may be a combination of only-noise and signal-plus-noise components, and the detection performance may be degraded. In this study, we assume that there is a single user in each frequency band and that the primary user signal has arrived at the CR receiver, before the CR starts sensing the spectrum (i.e., the primary user signal is either present or absent throughout the sensing duration of the CR). This is a widely used assumption in the literature, and is a valid assumption for the current study as the relative detection performance of joint and independent detection methods is of main interest. Next, modeling the decision variable using energy detection is explained.

2.1. Modeling the decision variable

Considering the received signals in (1) and (2), an energy detection scheme can be used [6]. Using a square-law detector and normalizing the output with the two-sided noise power spectral density $N_0/2$, the decision variable for the mth system can be obtained as

$$d_m = \frac{2}{N_0}\int_0^{T_m} \left|r_m(t)\right|^2 dt, \tag{3}$$

where T_m is the integration time for the mth system and $|\cdot|$ is the absolute value operator. Adopting the sampling theorem approximation used for bandpass signals in [6] and [10], the decision variable can be approximated as

$$d_m \approx \frac{1}{N_0 W_m}\sum_{i=1}^{T_m W_m}\left[\left(A_I s_I^{(i)} - A_Q s_Q^{(i)} + n_I^{(i)}\right)^2 + \left(A_I s_Q^{(i)} + A_Q s_I^{(i)} + n_Q^{(i)}\right)^2\right], \tag{4}$$

where $s_I^{(i)}$ and $n_I^{(i)}$ ($s_Q^{(i)}$ and $n_Q^{(i)}$) denote the ith samples of the low-pass equivalent in-phase (quadrature) components of $s_m(t-\tau_m)$ and $n_m(t)$, respectively, sampled at the Nyquist rate W_m, $A_I = A_m\cos\theta_m$, and $A_Q = A_m\sin\theta_m$ in the case of $H_{1,m}$. In the case of

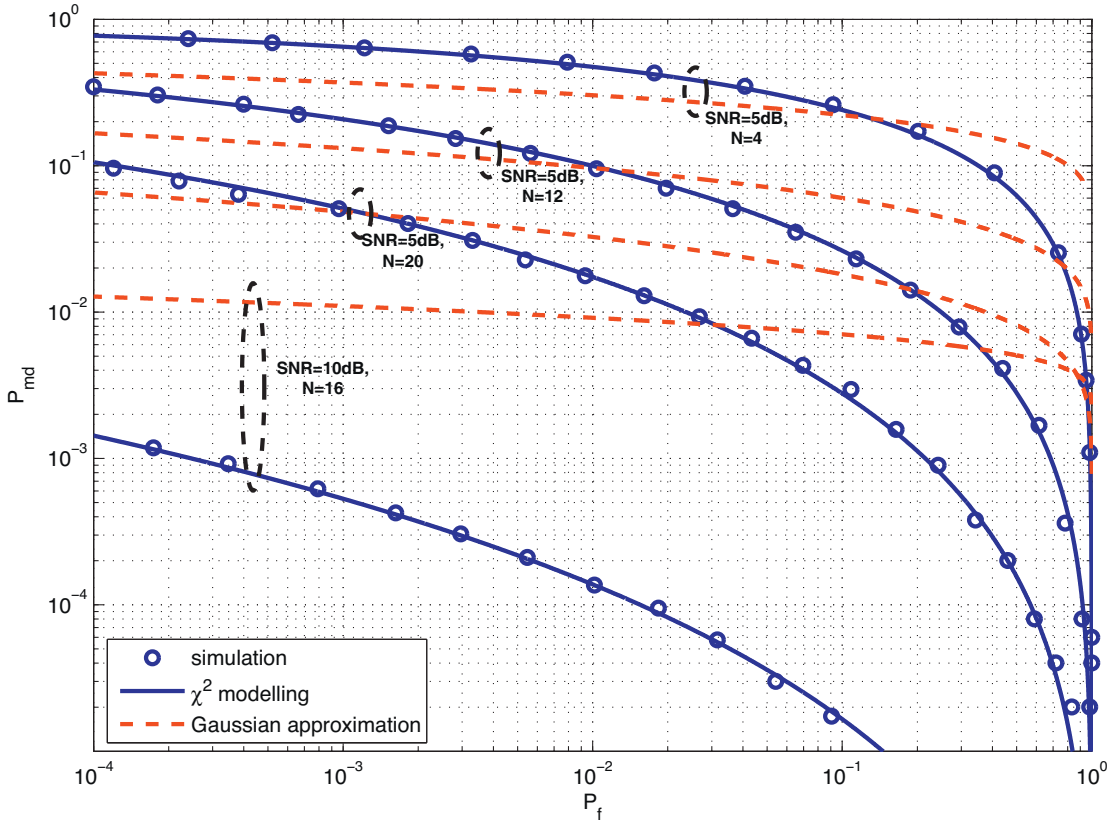

Fig. 1. Complimentary ROC curves in the presence of a primary system for various SNR and integration time-bandwidth product values.

$H_{0,m}$, only the noise terms, $n_I^{(i)}$ and $n_Q^{(i)}$, will determine the decision variable d_m in (4). Assuming that the samples of the primary signal, $s_I^{(i)}$ and $s_Q^{(i)}$, given in (4) are zero-mean Gaussian random variables,[1] the decision variable d_m will consist only of zero-mean Gaussian random variables in either hypothesis. Hence, under $H_{0,m}$ it can be shown that d_m can be modeled using χ^2 distribution with $N_m = 2T_mW_m$ degrees of freedom, where the variance term is $\sigma_m^2 = (\sigma_{n_m}^2)/(N_0W_m) = 1$ [17]. Similarly, under $H_{1,m}$, it can be shown that d_m can be modeled using χ^2 distribution with $N_m = 2T_mW_m$ degrees of freedom, where the variance term is $\sigma_m^2 = \gamma_m + 1$ with SNR defined as $\gamma_m = (A_m^2\sigma_s^2)/(N_0W_m)$ and σ_s^2 being the variance of the primary signal samples. Accordingly, the probability density function (pdf) of d_m for either hypothesis can be expressed as

$$f_{D_m}(d_m) = \frac{1}{\sigma_m^{N_m} 2^{N_m/2}\Gamma(N_m/2)} d_m^{N_m/2-1} e^{-d_m/2\sigma_m^2}, \quad (5)$$

where $\Gamma(a,b) = \int_b^\infty e^{-t}t^{a-1}dt$ is the upper incomplete Gamma function and $\Gamma(a) = \Gamma(a,0)$ is the Gamma function [22]. In [8] and [14], assuming large N_m, d_m was assumed to be normally distributed with $d_m \sim \mathcal{N}(N_m\sigma_m^2, 2N_m\sigma_m^4)$, where $\sigma_m^2 = 1$ for $H_{0,m}$ and $\sigma_m^2 = (\gamma_m + 1)$ for $H_{1,m}$. In the next subsection, we will discuss whether the χ^2 distribution or the normal distribution is more suitable for modeling the decision variable. Next, the detection of a single system is presented.

[1] For example, the samples of an orthogonal frequency-division multiplexing (OFDM) based primary signal sampled at the Nyquist rate can be well-approximated as independent and identically distributed (i.i.d.) zero-mean Gaussian random variables based on the central limit theorem [21].

2.2. Detection of a single system

In conventional detection, the decision variable d_m is compared to a pre-selected threshold value λ_m in order to make a decision for the mth system. The performance measures, probability of false alarm and probability of detection, can be respectively expressed as

$$P_{f,m} = \Pr[d_m > \lambda_m | H_{0,m}] \quad (6)$$

$$P_{d,m} = \Pr[d_m > \lambda_m | H_{1,m}], \quad (7)$$

where (6) and (7) can be simplified to

$$P_{x,m} = Q\left(\frac{N_m}{2}, \frac{\lambda_m}{2\sigma_m^2}\right) = \frac{\Gamma\left((N_m/2), (\lambda_m/2\sigma_m^2)\right)}{\Gamma(N_m/2)}, \quad x \in \{f, d\} \quad (8)$$

with the corresponding σ_m^2 values for $H_{0,m}$ and $H_{1,m}$, and $Q(a, b)$ is the regularized upper incomplete Gamma function [22]. If d_m was assumed to be normally distributed as in [8] and [14], then (8) simplifies to

$$P_{x,m} = Q\left(\frac{\lambda_m - N_m\sigma_m^2}{\sigma_m^2\sqrt{2N_m}}\right), \quad x \in \{f, d\} \quad (9)$$

with the corresponding σ_m^2 values for $H_{0,m}$ and $H_{1,m}$, and $Q(\cdot)$ is the Gaussian Q-function given as $Q(x) = (1/\sqrt{2\pi})\int_x^\infty e^{-t^2/2}dt$ [22]. In Fig. 1, complementary receiver operating characteristic (ROC) curves (i.e., P_f vs. $P_{md} = 1 - P_d$) are plotted to compare the theoretical performance according to (8) and (9) to a simulated primary system detected using a square-law detector according to (1)–(3), (6) and (7). The primary system is assumed to be a WiMAX-OFDM system as defined in [23] with further assumptions of quadrature phase-shift keying (QPSK) modulation, $K = 256$ subcarriers and

a system bandwidth of $W_1 = 8$ MHz being used. The integration times in (3) are selected as $T_1 = \{0.25, 0.75, 1, 1.25\}$ μs resulting in $N = \{4, 12, 16, 20\}$, and an SNR of $\gamma_1 = \{5, 10\}$ dB are assumed. It can be observed that the results for a χ^2 distributed d_1 matches the simulation results well even on a log-scale, whereas the normal distribution yields a good approximation in the linear-scale for low SNR only [8]. Since the system implementation requires very low P_f and P_{md} values, we need to monitor the changes in the log-scale. Therefore, we will build our model based on the accurate χ^2 distribution.

2.3. Detection of multiple systems

If the CR is a wideband system, then it has to assess the presence of all coexisting primary systems before it can communicate. Accordingly, the hypotheses have to be redefined as $\mathbf{H} = \left\{[H_{x_M,M}, \ldots, H_{x_2,2}, H_{x_1,1}] | x_m \in \{0, 1\}\right\}$. Since there are M primary systems, there are 2^M possible combinations of hypotheses. Accordingly, the CR can only transmit if $x_m = 0$, $\forall m$, which can be represented by $\mathbf{H}_0$. For the rest $2^M - 1$ combinations even if a single primary system is active, then the CR is not allowed to communicate. The hypotheses corresponding to having at least one active system can be represented by $\mathbf{H}_{1,i}$, $1 \le i \le 2^M - 1$, where the active and passive systems in each hypothesis can be determined by the relation

$$i = (x_M \cdots x_2 x_1)_2 \tag{10}$$

with $(\cdot)_2$ denoting the base-2 representation of i. Hence, the probability of false alarm and probability of detection for multiple systems can be expressed as

$$P_f = 1 - \Pr\left[\bigcap\nolimits_{m=1}^{M} (d_m < \lambda_m) \,\middle|\, \mathbf{H}_0\right] \tag{11}$$

$$P_d = 1 - \sum_{i=1}^{2^M-1} \Pr\left[\bigcap\nolimits_{m=1}^{M} (d_m < \lambda_m) \,\middle|\, \mathbf{H}_{1,i}\right] \Pr\left[\mathbf{H}_{1,i} \,\middle|\, \mathbf{H}_1\right], \tag{12}$$

where $\mathbf{H}_1 = \bigcup_{i=1}^{2^M-1} \mathbf{H}_{1,i}$.

The probability of detection expression given in (12) is different from the conventional expression mainly due to the probability term being conditioned on different hypotheses, $\mathbf{H}_{1,i}$. Hence, the probabilities of these hypotheses are important in determining (12). Accordingly, the probability that all the primary systems are passive is $p_0 = \Pr[\mathbf{H}_0]$, whereas $p_i = \Pr[\mathbf{H}_{1,i}]$, $1 \le i \le 2^M - 1$, is the probability that $\mathbf{H}_{1,i}$ holds, where $\sum_{i=0}^{2^M-1} p_i = 1$. For example, if there are $M = 4$ interdependent systems and p_7 is close to unity, that means the first three systems are jointly active most of the time while the fourth system is not active (i.e., $7 = (0\,1\,1\,1)_2$). To note, the probabilities $\{p_i\}$ can also be referred to as joint system activity values.

In Section 3, probability of false alarm and detection expressions given in (11) and (12) will be adapted for joint and independent detection methods, and exact expressions for these probabilities will be obtained.

2.4. Operation capability

In addition to probabilities of false alarm and detection, it is also important to assess how the wideband CR will be able to utilize the common band. Accordingly, we define

$$T_u = p_0(1 - P_f) \tag{13}$$

$$T_h = (1 - p_0)(1 - P_d) \tag{14}$$

as additional performance measures, where T_u and T_h are the fractions of time the wideband cognitive radio is operating usefully and harmfully (causing interference to primary systems), respectively. It should be noted that the fraction of time during which the cognitive radio is not operating, T_n, is given by $T_n = 1 - T_u - T_h$.

3. Detection methods

In the following, we consider the implementation of two detection methods for $M > 2$ primary systems that are interdependent. For both methods, it is assumed that the systems' joint activity values $\{p_i\}$ and the pdfs of the decision variables $\{d_m\}$ are known a priori. This is a reasonable assumption as the traffic information of the primary systems may be available to secondary users, and the SNR of the primary signals can be estimated at the receiver.

3.1. Joint detection

Knowing $\{p_i\}$ and the pdfs of $\{d_m\}$, the MAP decision rule serves as an optimal decision rule. The hypothesis can be estimated by finding the maximum of the MAP decision metrics as

$$\begin{aligned} &\hat{i} = \underset{i \in \{0,1,\ldots,2^M-1\}}{\operatorname{argmax}} \; PM_i \\ &\hat{\mathbf{H}} = \mathbf{H}_0 \text{ if } \hat{i} = 0; \quad \hat{\mathbf{H}} = \mathbf{H}_1 \text{ if } \hat{i} = \{1, 2, \ldots, 2^M - 1\}, \end{aligned} \tag{15}$$

where the decision metrics are $PM_0 = b_0 p_0 f_{D_1,D_2,\ldots,D_M|\mathbf{H}_0}(d_1, d_2, \ldots, d_M)$ and $PM_i = b_i p_i f_{D_1,D_2,\ldots,D_M|\mathbf{H}_{1,i}}(d_1, d_2, \ldots, d_M)$, $\{i = 1, 2, \ldots, 2^M - 1\}$. The bias terms $\{b_i | i = 0, 1, 2, \ldots, 2^M - 1\}$ are the intentionally introduced terms to achieve a desired trade-off between the probabilities of false alarm and detection, and $f_{D_1,D_2,\ldots,D_M|\mathbf{H}_x}(d_1, d_2, \ldots, d_M)$ are the joint pdfs conditioned on the hypothesis $\mathbf{H}_x$. Since the primary systems are in non-overlapping frequency bands, the joint pdfs conditioned on $\mathbf{H}_x$ can be expressed using (5) as

$$\begin{aligned} f_{D_1,D_2,\ldots,D_M|\mathbf{H}_x}(d_1, d_2, \ldots, d_M) &= \prod_{m=1}^{M} \left(\frac{d_m^{N_m/2-1}}{2^{N_m/2}\Gamma(N_m/2)}\right) \\ &\times \left(\frac{e^{-d_m/2\sigma_m^2}}{(\sigma_m^2)^{N_m/2}}\right) = C\prod_{m=1}^{M} \left(\frac{e^{-d_m/2\sigma_m^2}}{(\sigma_m^2)^{N_m/2}}\right), \end{aligned} \tag{16}$$

where $C = \prod_{m=1}^{M} \left((d_m^{N_m/2-1})/(2^{N_m/2}\Gamma(N_m/2))\right)$ is a common term for all joint pdfs independent of the hypotheses. On the other hand, the second term in brackets depends on the hypothesis it is conditioned on, as the variance term defined before (5) is $\sigma_m^2 = \gamma_m + 1$ for $H_{1,m}$ and $\sigma_m^2 = 1$ for $H_{0,m}$. Accordingly, using the relation of the index i with $\{x_m | m = 1, 2, \ldots, M\}$ as given in (10), the decision metrics can be written as

$$\begin{aligned} &PM_i = b_i p_i C \prod_{m=1}^{M} \frac{\exp\left((-d_m)/(2(\gamma_m + 1)^{x_m})\right)}{(\gamma_m + 1)^{x_m N_m/2}}, \\ &\left\{i = 0, 1, 2, \ldots, 2^M - 1\right\} \end{aligned} \tag{17}$$

Considering (11), (12) and (15), the probabilities of false alarm and detection can be redefined as

$$P_f = 1 - \Pr\left[\bigcap\nolimits_{i=1}^{2^M-1} (PM_0 < PM_i) \,\middle|\, \mathbf{H}_0\right] \tag{18}$$

$$P_d = 1 - \sum_{i=1}^{2^M-1} \frac{p_i}{1-p_0} \Pr\left[\bigcap\nolimits_{j=1}^{2^M-1} (PM_0 < PM_j) \,\middle|\, \mathbf{H}_{1,i}\right]. \quad (19)$$

By substituting (17) into the comparison term $\{PM_0 > PM_i\}$, (18) and (19) can be simplified to

$$P_f = 1 - P_{cond,\mathbf{H}_0}\left[\prod_{m=1}^{M}(1-P_{f,m})\right] \quad (20)$$

$$P_d = 1 - \sum_{i=1}^{2^M-1} \frac{p_i}{1-p_0} P_{cond,\mathbf{H}_{1,i}}\left[\prod_{m=1}^{M}(1-P_{d,m})^{Xm}(1-P_{f,m})^{(1-x_m)}\right], \quad (21)$$

where $P_{cond,\mathbf{H}_x}$, $\{x=0\}$ or $\{x=1,i\}$ is the conditional probability term obtained as

$$P_{cond,\mathbf{H}_x} = \prod_{i=1}^{2^M-1} P_{\lambda_i|(\lambda_1)^{x_1},(\lambda_2)^{x_2},\ldots,(\lambda_{2^{m-1}})^{xm},\ldots,(\lambda_{2^{M-1}})^{x_M},\mathbf{H}_x} \quad (22)$$

with

$$P_{\lambda_i|(\lambda_1)^{x_1},\ldots,(\lambda_{2^{M-1}})^{x_M},\mathbf{H}_x} = \Pr\left[\sum_{m=1}^{M} x_m a_m d_m < \lambda_i \,\middle|\, x_1 a_1 d_1 < \lambda_1, \ldots, x_M a_M d_M < \lambda_{2^{M-1}}, \mathbf{H}_x\right] \quad (23)$$

and $a_m = \gamma_m/(2(\gamma_m+1))$. The resulting threshold values are

$$\lambda_i = \left[\sum_{m=1}^{M} \frac{x_m N_m}{2} \ln(\gamma_m+1) + \ln\left(\frac{p_0}{p_i}\right) + \ln\left(\frac{b_0}{b_i}\right)\right] \quad (24)$$

for $i=\{1,2,\ldots,2^M-1\}$, where $\{x_m\}$ are obtained from (10). It should be noted that $\left\{\lambda_{2^{m-1}} | m=1,2,\ldots,M\right\}$ correspond to independent threshold values[2] for each band, m, whereas the rest of the $\{\lambda_i\}$ values (i.e., 2^M-M-1 values) correspond to the joint bands. For example, when $M=4$ the threshold λ_5 corresponds to bands 1 and 3 (i.e., $5=(0101)_2$). We calculate the probabilities of false alarm and detection using (20) and (21), where the terms in (22) can be calculated numerically as explained in Appendix A. By letting $b_1 = b_2 = \cdots = b_{2^M-1} = b$ in (24), and varying the value of b, a tradeoff between (P_f, P_d)-pairs can be obtained with a close-to-optimal performance [17].

3.2. Independent detection

The probabilities of false alarm and detection for multiple bands can be expressed as

$$P_f = 1 - \prod_{m=1}^{M}(1-P_{f,m}) \quad (25)$$

$$P_d = 1 - \sum_{i=1}^{2^M-1} \frac{p_i}{1-p_0} \prod_{m=1}^{M}(1-P_{d,m})^{x_m}(1-P_{f,m})^{(1-x_m)} \quad (26)$$

if the bands are independently processed. These equations can also be obtained by letting $P_{cond,\mathbf{H}_x} = 1$ in (20) and (21).

[2] Note that these values resulting from MAP detection and corresponding to the mth band are different from the conventional threshold values $\{\lambda_m | m=1,2,\ldots,M\}$ given in (11) and (12).

3.2.1. NP test

In order to obtain the best detection performance the NP test can be employed, which optimizes the threshold values in order to maximize P_d for a given target $P_f=\alpha$:

$$\max_{\{\lambda_{2^{m-1}}|m=1,2,\ldots,M\}} P_d \quad s.t.\ P_f = \alpha. \quad (27)$$

Here, $\left\{\lambda_{2^{m-1}} | m=1,2,\ldots,M\right\}$ are the independent threshold values to be optimized. This is equivalent to maximizing P_d over an M-dimensional search space. In Fig. 2, possible (P_f, P_{md})-pairs that are obtained by using $\lambda_1 \in [0,100]$ and $\lambda_2 \in [0,100]$ in (25) and (26), i.e., the search space for independent detection, and the numerically calculated minimum P_{md} values for fixed $P_f=\{\alpha\}$ are plotted when $M=2$ with $P:\{p_0=0.76, p_1=0.06, p_2=0.11, p_3=0.07\}$, $N_1=24$, $N_2=8$, $\gamma_1=5$ dB, and $\gamma_2=10$ dB. It can be observed that, as expected, the best (P_f, P_{md})-pairs are obtained by the NP test as the curve attains the lower bound of the search space. For larger values of M, the computation complexity of the NP test increases.

3.2.2. MAP test

Alternatively, we consider using the threshold values obtained from MAP detection instead of the NP test. These threshold values indeed result from the $\{PM_0 > PM_i\}$ comparisons, and serve intrinsically as posterior odds ratios [24]. Moreover, these values are easier to compute compared to the NP test. Accordingly, the threshold values that will be used in (25) and (26) can be obtained from (23) and (24) by letting the index of λ_i as $i=2^{m-1}$ for $m=\{1,2,\ldots,M\}$ independent bands, and using the resulting relation

$$i = 2^{m-1} = (x_M \cdots x_{m+1} x_m x_{m-1} \cdots x_1)_2 = (0\ldots010\ldots0)_2, \quad (28)$$

where x_m is the only non-zero term. Note that the threshold values $\{\lambda_i\}$ given in (23) for joint detection are related to decision variables $\{d_m\}$ multiplied by the term a_m. Therefore, the threshold values for each independent band can be obtained as

$$\lambda_{2^{m-1}} = \left[\frac{N_m}{2}\ln(\gamma_m+1) + \ln\left(\frac{p_0}{p_{2^{m-1}}}\right) + \ln\left(\frac{b_0}{b_{2^{m-1}}}\right)\right] \Big/ a_m \quad (29)$$

for $m=\{1,2,\ldots,M\}$. In Appendix B, the derivation of $\left\{\lambda_{2^{m-1}}\right\}$ is presented in more detail by using the comparisons $\left\{PM_0 < PM_{2^{m-1}}\right\}$. Similar to joint detection, by letting $b_1 = b_2 = \cdots = b_{2^M-1} = b$ in (29) and varying it, a tradeoff between (P_f, P_d)-pairs can be obtained.

4. Results

In this section, we initially provide simulation and numerical results to confirm the validity of the joint detection model and the independent detection model that uses the threshold values obtained from MAP detection when $M>2$. We then provide some numerical results to determine the gain of joint detection over independent detection in terms of various system parameters such as the effects of joint system activity values, number of interdependent systems and SNR. Finally, we present the operation capability of CRs for practical scenarios. For all scenarios, it is assumed that $\Pr[\mathbf{H}_0]=0.90$ and $\Pr[\mathbf{H}_1]=0.10$. Also, SNR and N values for each band are fixed to 10 dB and 8, respectively, unless otherwise indicated.

In Fig. 3, we validate the probabilities of false alarm and detection expressions given in (20) and (21) for joint detection. Accordingly, we simulate the decision metrics $\{PM_i\}$ and evaluate them in (18) and (19) to obtain the complementary ROC curves. The system activity values considered are $P_1:\{p_{2^M-1}=0.1, p_1=p_2=\ldots=p_{2^M-2}=0\}$ and $P_2:\{\text{random } p_i\}$ for various SNR and N values when $M=3$ and $M=4$. It can be observed that the simulation results confirm the validity of the joint detection model.

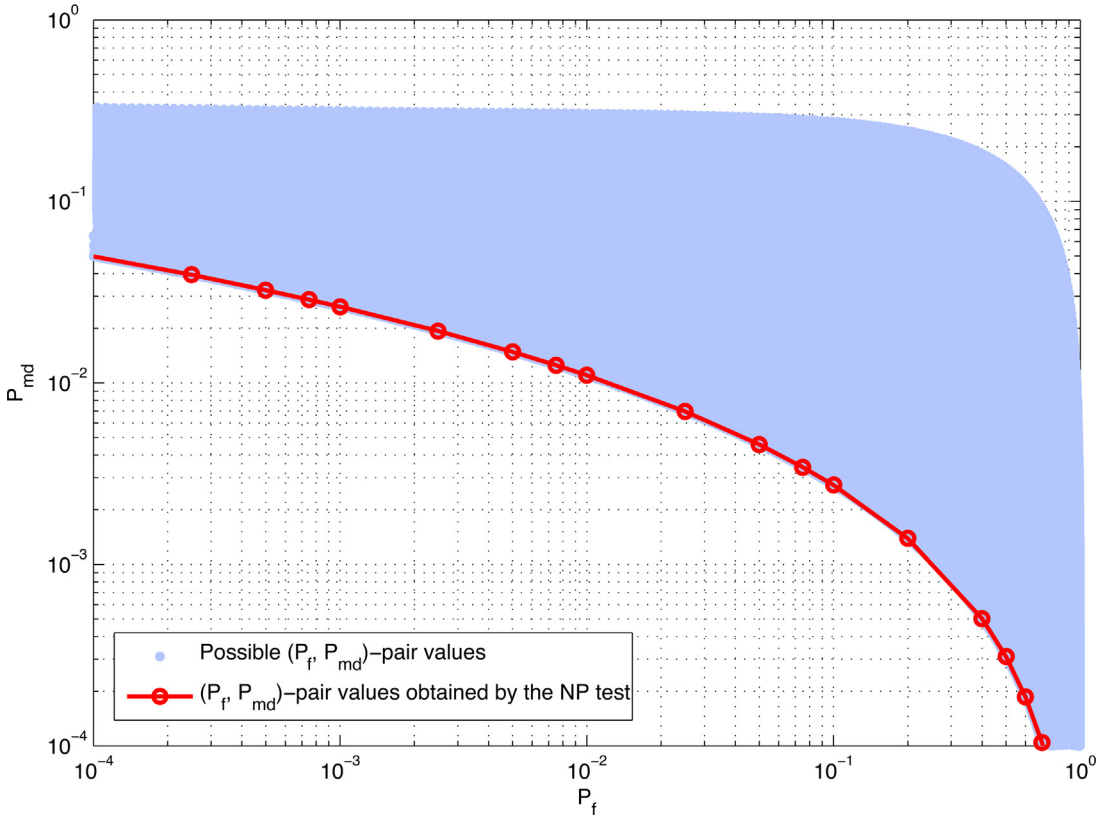

Fig. 2. The (P_f, P_{md})-pair search space and the (P_f, P_{md})-pairs obtained by the NP test when P: $\{p_0 = 0.76, p_1 = 0.06, p_2 = 0.11, p_3 = 0.07\}$, $N_1 = 24$, $N_2 = 8$, $SNR_1 = 5$ dB and $SNR_2 = 10$ dB.

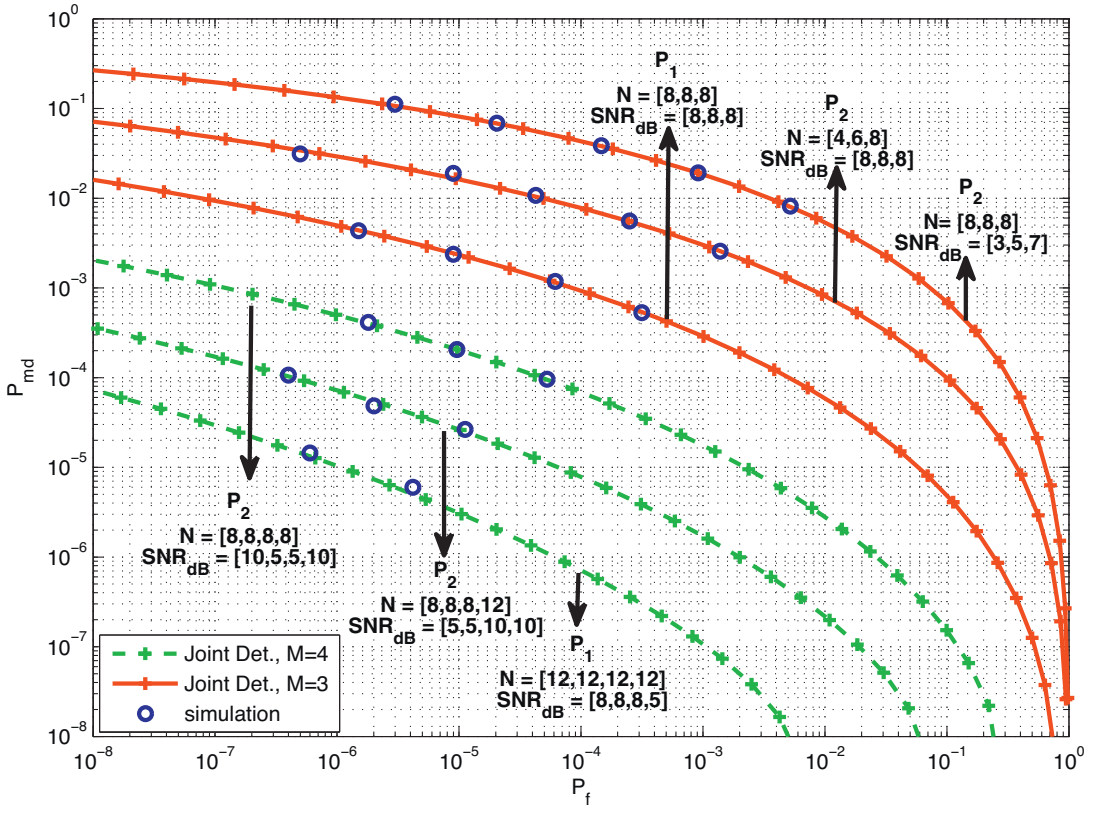

Fig. 3. Validating the complimentary ROC curves of joint detection for various P, N, SNR and M values.

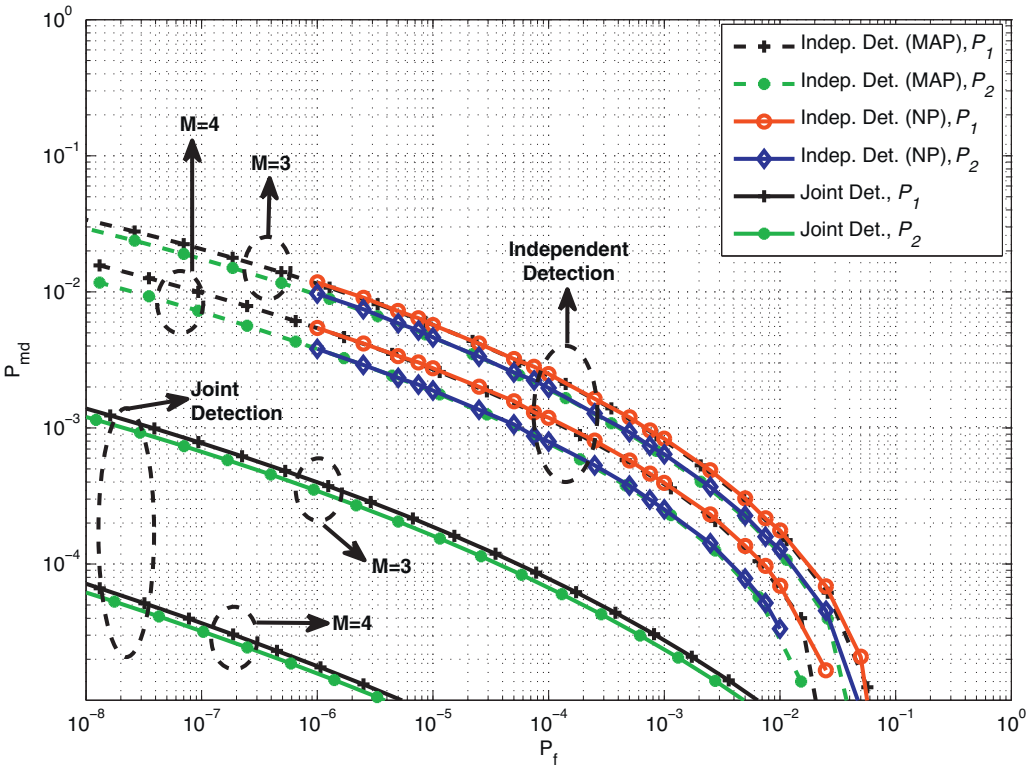

Fig. 4. Complimentary ROC curves of joint and independent detection for various P and M values.

In Fig. 4, we present joint and independent detection performances on the same complementary ROC plot. For that, we consider two different sets of system activity values, $P_1 : \{p_{2^M-1} = 0.07, p_1 = p_2 = p_4 = \ldots = p_{2^{M-1}} = 0, p_i\}$ and $P_2 : \{p_{2^M-1} = 0.08, p_1 = p_2 = p_4 = \ldots = p_{2^{M-1}} = 0, p_i\}$ for $M = 3$ and $M = 4$, where p_i represent the probability of jointly active bands and have equal values, $p_i = (0.10 - p_{2^M-1})/(2^M - M - 2)$, $\forall i$. It can be observed that the joint detection performs better than the

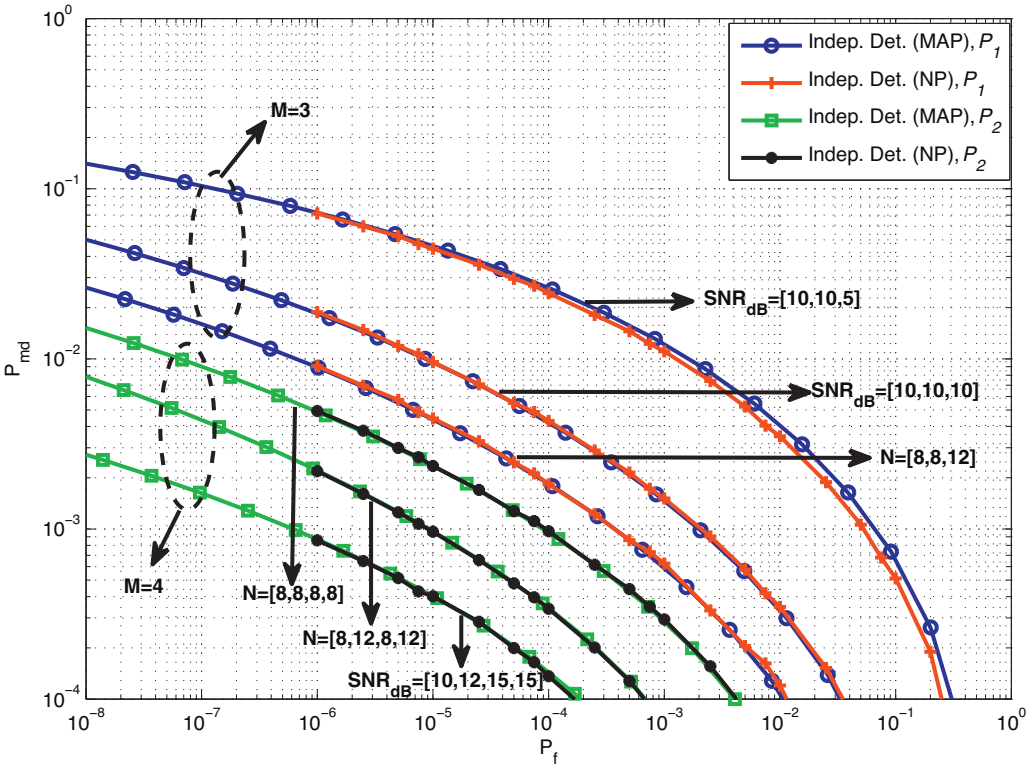

Fig. 5. Validating the complimentary ROC curves of independent detection for various P, N, SNR and M values.

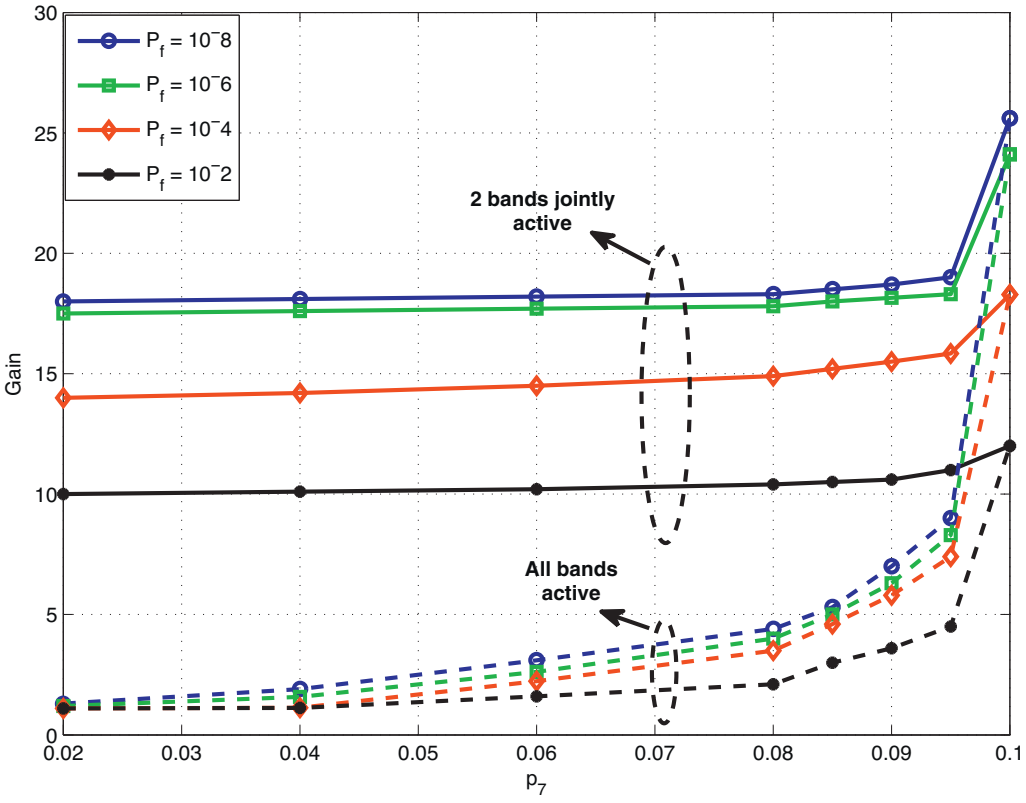

Fig. 6. The effect of system activity values on the detection performance when $M = 3$.

independent detection with M increasing and for P_2 (all M bands are active more frequently) as expected. Also, it is important to note that the threshold values obtained by MAP detection and used in independent detection achieve the same performance as the NP test results. In Fig. 5, we further validate the independent detection results for various SNR and N values, when two different sets of randomly selected joint system activity values (P_1 for $M = 3$ and P_2 for $M = 4$) are used. Considering that the performance results are coinciding, the MAP test based approach can be used with an easier implementation to replace the NP test for independent detection.

Next, we quantify the gain of joint detection over independent detection for various scenarios. The gains are defined as the P_{md} ratios of independent and joint detection at fixed P_f values, i.e., $Gain = (P_{md}(indep.))\,/\,(P_{md}(joint))$. This is an important performance measure from the perspective of a primary user because the ratio indicates how much more the primary user will be interfered by the CR if independent detection is used instead of the joint detection. In Fig. 6, misdetection performance gains are compared at various P_f values for 2-band jointly active (i.e., only $\{p_3, p_5, p_6\}$ are non-zero) and all-band active (i.e., $\{p_1, p_2, \cdots, p_6\}$ are non-zero) cases when $M = 3$ and p_7 varying. The probability value $(0.10 - p_7)$ is equally distributed among the non-zero probability values for both cases. It can be observed that the gains increase with P_f decreasing and p_7 increasing. When $p_7 = 0.1$, the performances for both cases merge at the best gain value.

In Fig. 7, the effect of SNR degradation on the detection performance is investigated for various M values. Again, the misdetection gain values are calculated at various P_f values. For each case, we assume that all systems are jointly active all the time, i.e., $p_{2^M-1} = 0.1$, for $M = \{2, 3, 4\}$. When $M = 2$, gains similar to the ones reported in [17] are obtained. When M is increased, there is a significant increase in gain due to processing the bands jointly. When the SNR decreases in a band, the $M = 4$ case can compensate better due to other active bands having significant SNR values.

Finally, the operation capabilities of CRs are considered. Accordingly, curves which show the fractions of time the CR is operating usefully and harmfully are plotted using (13) and (14) for various scenarios. In Fig. 8, the effect of system activity values on the operation times of CRs is investigated when the SNR of each band is $\{5, 10\}$ dB when $M = 3$. The joint system activity values are non-zero only for p_0 and p_7 for three different sets. Since the P_f and P_d values obtained from (11) and (12) are conditioned on $\mathbf{H}_0$ and $\mathbf{H}_1$, the detection performances of all three cases are the same. However, their operation capabilities are different as can be deduced from (13) and (14), and as plotted in Fig. 8. When $p_0 = 0.6$, $p_7 = 0.4$, and SNR = 5 dB, by selecting appropriate bias values for joint detection the CR can operate at point **C**, where it can usefully operate almost 60% of the time while interfering with the primary system only 0.3% of the time. On the other hand, using independent detection with appropriate threshold values, the CR can operate at point **D** almost 60% of the time usefully while interfering with the primary system 1.8% of the time. If the interference level is restricted to a certain amount by the primary system, then the CR operation points for either detection can be determined accordingly (e.g., operating at points **A** or **B** if $T_h = 10^{-4}$ is allowed).

In Fig. 9, the operation capabilities of CRs are investigated for $P_1 : \{p_0 = 0.9,\ p_7 = 0.1\}$ (i.e., full gain), $P_2 : \{p_0 = 0.9,\ p_7 = 0.05,\ p_3 = p_5 = p_6 = 0.05/3\}$ (i.e., joint bands active), and $P_3 : \{p_0 = 0.9,\ p_7 = 0.05, p_1 = p_2 = \cdots = p_6 = 0.05/6\}$ (i.e., all bands active) when $M = 3$. The gains of these cases can be observed in Fig. 6. Since $p_0 = 0.9$, the CR can operate usefully at most 90%. Therefore, particularly the region where the CR can operate usefully with high utilization of the common band is zoomed in. When T_u is 89.99%, the interfering time of CR due to independent detection is approximately 18 and 14 times the interfering time due to joint detection for P_1 and

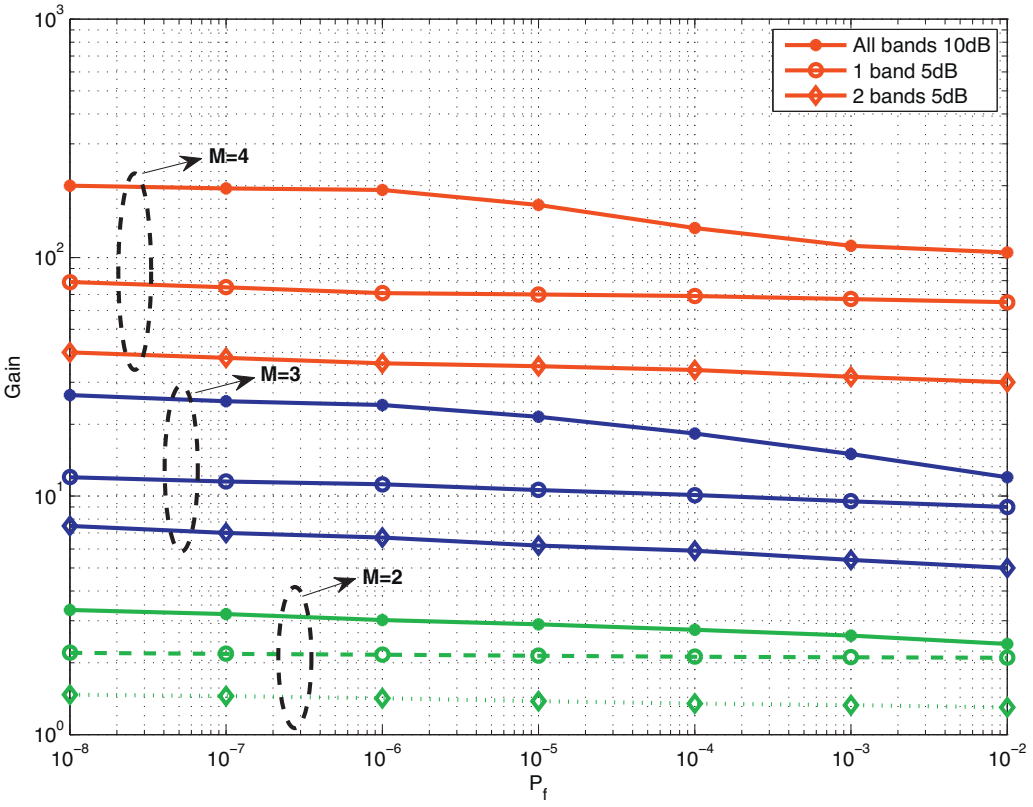

Fig. 7. The effect of SNR values on the detection performance for various M values.

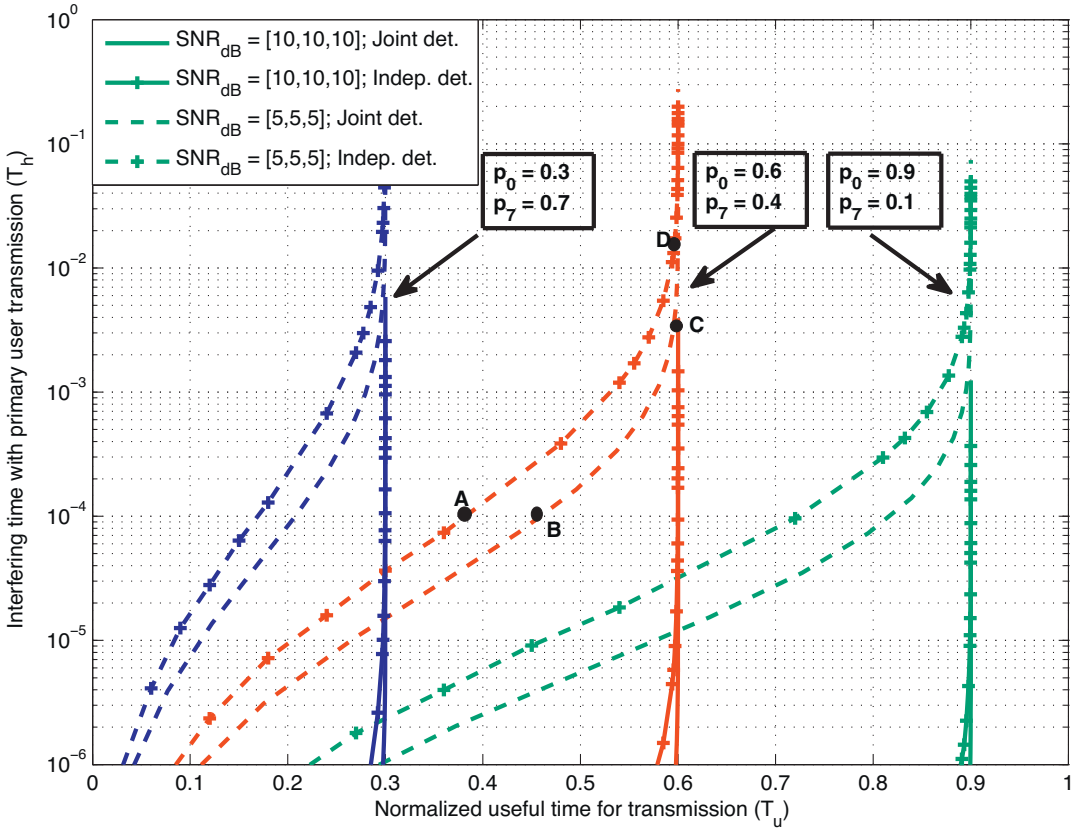

Fig. 8. Fractions of time the cognitive radio is operating usefully and harmfully for $SNR = \{5, 10\}$ dB and various system activity values.

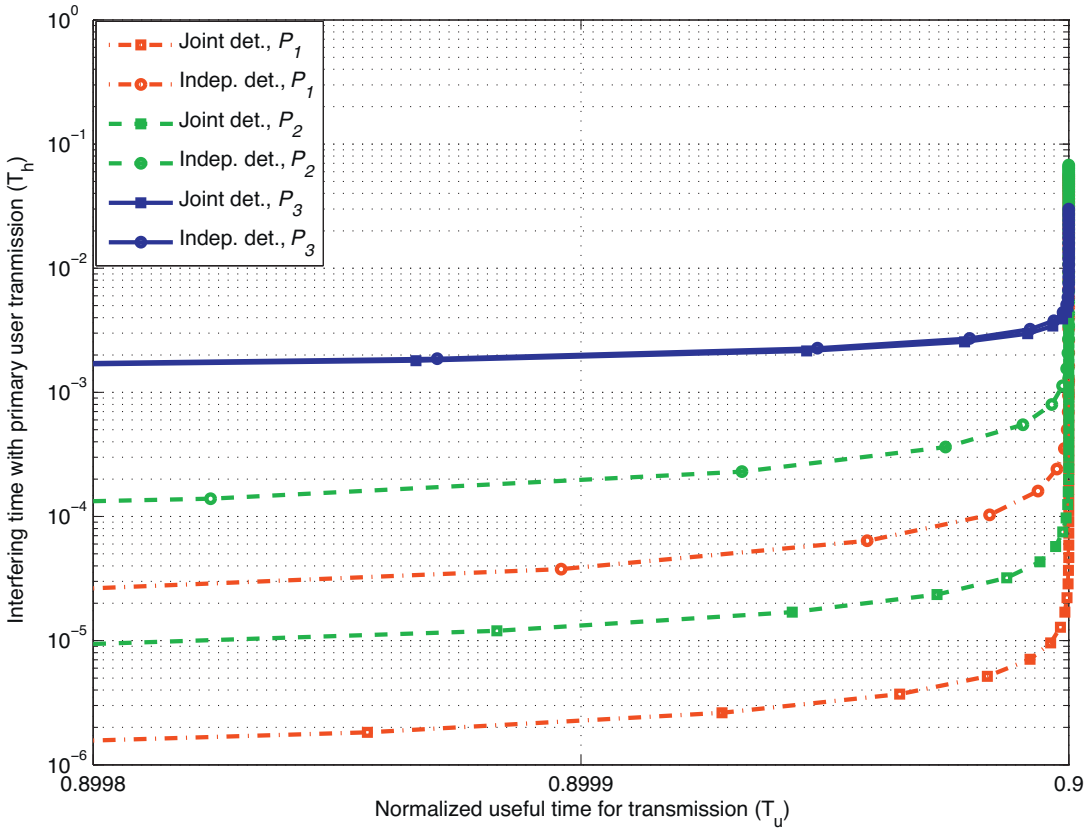

Fig. 9. The effect of system activity values on the fractions of time the cognitive radio is operating usefully and harmfully.

P_2, respectively, whereas the performances for P_3 are similar. These results are also in correspondence with the gains provided in Fig. 6.

While the current study presented complementary ROC curves and operation capabilities of CRs for the comparison of joint and independent detection methods from the detection perspective of a wideband CR, the implementation may require each primary user having a constraint on the interference level. Accordingly, studying the CR throughput subject to some interference constraints defined for each user as in [14] may be an interesting extension of the current work, however, is a research topic for future study.

5. Conclusion

In this paper, we studied the primary system detection performance of a wideband CR assuming that there are multiple ($M>2$) coexisting primary systems and that these primary systems may be jointly active. Accordingly, we considered the implementation of joint and independent detection methods. For the joint detection, we considered a MAP based detection that intrinsically optimizes the threshold values. For the independent detection, we considered the implementation of the optimum NP test based detection, and a simpler implementation that uses the threshold values obtained from the MAP detection, where both methods were shown to perform the same. We confirmed the validity of the joint detection model and the MAP based independent detection model using simulation studies. We then provided numerical examples to quantify the performance gain of joint detection over independent detection. Finally, we presented the operation capabilities of CRs in terms of the fractions of time they can operate usefully and harmfully. The results presented are important for the practical implementation of multiband detection when there are multiple primary systems that are known to be interdependent.

Acknowledgements

This work was supported by a Marie Curie International Reintegration Grant within the 7^{th} European Community Framework Programme.

Appendix A. Numerical evaluation of the conditional probability term

The conditional probability terms $\left\{P_{\lambda_i|(\lambda_1)^{x_1},\ldots,(\lambda_{2^{M-1}})^{x_M},\mathbf{H}_x}\right\}$ in (22) can be numerically computed conditioned on $\mathbf{H}_x$ for given i and M. For known i and M values, initially $\{x_i\}$ can be obtained from the relation $i=(x_M \ldots x_2 x_1)_2$. Then the expression in (23) can be simplified as

$$\Pr[d' < \lambda_i|\mathbf{H}_x], \tag{30}$$

where the variable d' has a pdf

$$f_{D'}(d') = f_{D'_1}(d'_1) * f_{D'_2}(d'_2) * \ldots * f_{D'_M}(d'_M) \tag{31}$$

with $*$ representing the convolution operator and each pdf $f_{D'_m}(d'_m)$ obtained from (5) as

$$f_{D'_m}(d'_m) = \frac{f_{D_m}(d'_m/a_m)/a_m}{1 - Q\left((N_m/2), ((\lambda_{2^{m-1}})/(2a_m\sigma_m^2))\right)}, \quad 0 < d'_m < \lambda_{2^{m-1}}, \tag{32}$$

if $x_m = 1$, $m \in \{1, 2, \ldots, M\}$. Otherwise, if $x_m = 0$, $f_{D'_m}(d'_m) = \delta(d'_m)$, where $\delta(\cdot)$ is a Dirac delta function. For known $\{\lambda_i\}$ values that can be obtained from (24), the conditional probability term can be numerically computed using (30).

Appendix B. Derivation of the threshold values for independent detection

Considering the MAP decision metrics $\{PM_i\}$, probabilities of false alarm and detection for the mth system, $P_{f,m}$ and $P_{d,m}$, given in (6) and (7) can be written in terms of metric comparisons as

$$\begin{aligned} P_{x,m} &= \Pr[d_m > \lambda_{2^{m-1}} \,|H_{\{0,1\},m}\,] \\ &= \Pr[PM_0 < PM_{2^{m-1}} \,|H_{\{0,1\},m}\,], \quad x \in \{f, d\}. \end{aligned} \tag{33}$$

The probability term in (33) can also be written as $\Pr\left[\left((PM_0)/(PM_{2^{m-1}})\right) < 1 \,|H_{\{0,1\},m}\right]$. Since $i = 2^{m-1} = (x_M \cdots x_{m+1} x_m x_{m-1} \cdots x_1)_2 = (0 \cdots 010 \cdots 0)_2$ for the mth system, the ratio $(PM_0)/(PM_{2^{m-1}}) < 1$ can be simplified using (17) as

$$\frac{PM_0}{PM_{2^{m-1}}} = \left(\frac{b_0}{b_{2^{m-1}}}\right)\left(\frac{p_0}{p_{2^{m-1}}}\right)\left(\frac{e^{-d_m/2}}{e^{-d_m/2(\gamma_m+1)}}\right)(\gamma_m+1)^{N_m/2} < 1 \tag{34}$$

Taking the ln of both sides, (34) becomes

$$\frac{N_m}{2}\ln(\gamma_m+1) + \ln\left(\frac{p_0}{p_{2^{m-1}}}\right) + \ln\left(\frac{b_0}{b_{2^{m-1}}}\right) - d_m\left(\frac{\gamma_m}{2(\gamma_m+1)}\right) < 0. \tag{35}$$

Eq. (35) can be rearranged and used in (33) as $\Pr[d_m > \lambda_{2^{m-1}} \,|H_{\{0,1\},m}\,]$, where

$$\lambda_{2^{m-1}} = \left[\frac{N_m}{2}\ln(\gamma_m+1) + \ln\left(\frac{p_0}{p_{2^{m-1}}}\right) + \ln\left(\frac{b_0}{b_{2^{m-1}}}\right)\right] \Big/ a_m \tag{36}$$

as given in (29) and $a_m = \gamma_m/2(\gamma_m+1)$.

References

[1] Mitola J, Maguire GQ. Cognitive radio: making software radios more personal. IEEE Personal Commun 1999;6:13–8.
[2] Win MZ, Scholtz RA. Ultra-wide bandwidth time-hopping spread-spectrum impulse radio for wireless multiple-access communications. IEEE Trans Commun 2000;48:679–91.
[3] European Commission. Commission Decision of 21 April 2009 amending Decision 2007/131/EC on allowing the use of the radio spectrum for equipment using ultra-wideband technology in a harmonised manner in the Community. Official Journal of European Union 2009;L109:9–13.
[4] Yücek T, Arslan H. A survey of spectrum sensing algorithms for cognitive radio applications. IEEE Commun Surveys Tutorials 2009;11:116–30.
[5] Quan Z, Cui S, Poor HV, Sayed AH. Collaborative wideband sensing for cognitive radios. IEEE Signal Proc Mag 2008;25:60–73.
[6] Urkowitz H. Energy detection of unknown deterministic signals. IEEE Proc 1967;55:523–31.
[7] Ghasemi A, Sousa ES. Collaborative spectrum sensing for opportunistic access in fading environments. In: IEEE Proc DySPAN. 2005. p. 131–6.
[8] Mishra SM, Brodersen RW. Cognitive technology for improving ultra-wideband (UWB) coexistence. In: IEEE Proc ICUWB. 2007. p. 253–8.
[9] Zhang W, Mallik RK, Letaief KB. Optimization of cooperative spectrum sensing with energy detection in cognitive radio networks. IEEE Trans Wireless Commun 2009;8:5761–6.
[10] Digham FF, Alouini MS, Simon MK. On the energy detection of unknown signals over fading channels. IEEE Trans Commun 2007;55:21–4.
[11] Pandharipande A, Linnartz JPMG. Performance analysis of primary user detection in a multiple antenna cognitive radio. In: IEEE Proc ICC. 2007. p. 6482–6.
[12] Ma J, Zhou X, Li GY. Probability-based periodic spectrum sensing during secondary communication. IEEE Trans Commun 2010;58:1291–301.
[13] Erküçük S, Lampe L, Schober R. Analysis of interference sensing for DAA UWB-IR systems. In: IEEE Proc ICUWB. 2008. p. 17–20.
[14] Quan Z, Cui S, Sayed AH, Poor HV. Optimal multiband joint detection for spectrum sensing in cognitive radio networks. IEEE Trans Signal Proc 2009;57:1128–40.
[15] Khalid L, Raahemifar K, Anpalagan A. Cooperative spectrum sensing for wideband cognitive OFDM radio networks. In: IEEE Proc VTC-Fall. 2009. p. 1–5.
[16] Paysarvi-Hoseini P, Beaulieu NC. Optimal wideband spectrum sensing framework for cognitive radio systems. IEEE Trans Signal Proc 2011;59:1170–82.
[17] Erküçük S, Lampe L, Schober R. Joint detection of primary systems using UWB impulse radios. IEEE Trans Wireless Commun 2011;10:419–24.
[18] Yılmaz B, Erküçük S. Detection of jointly active primary systems. In: Future Network & Mobile Summit. 2012. p. 1–8.
[19] Sahin ME, Guvenc I, Arslan H. Opportunity detection for OFDMA-based cognitive radio systems with timing misalignment. IEEE Trans Wireless Commun 2009;8:5300–13.
[20] Wu JY, Wang CH, Wang TY. Performance analysis of energy detection based spectrum sensing with unknown primary signal arrival time. IEEE Trans Commun 2011;59:1779–84.
[21] Snow C, Lampe L, Schober R. Impact of WiMAX interference on MB-OFDM UWB systems: analysis and mitigation. IEEE Trans Commun 2009;57:2818–27.
[22] Abramowitz M, Stegun I. Handbook of mathematical functions. New York: Dover; 1964.
[23] IEEE Std 802.16-2004. Part 16: air interface for fixed broadband wireless access systems; 2004.
[24] Berger JO. Statistical decision theory: foundations, concepts, and methods. New York: Springer; 1980.